ICANS-XIII
13th Meeting of the International Collaboration on
Advanced Neutron Sources
October 11-14, 1995
Paul Scherrer Institut, 5232 Villigen PSI, Switzerland

THE PERFORMANCE OF NEUTRON SPECTROMETERS AT A LONG-PULSE SPALLATION SOURCE

Roger Pynn and Luc Daemen
Los Alamos National Laboratory, Los Alamos, New Mexico 87545, USA

ABSTRACT

At a recent workshop at Lawrence Berkeley National Laboratory [1], members of the international neutron scattering community discussed the performance to be anticipated from neutron scattering instruments installed at a 1 MW long-pulse spallation source (LPSS). Although the report of this workshop is long, its principal conclusions can be easily summarised and almost as easily understood. This article presents such a synthesis for a 60 Hz LPSS with 1 msec proton pulses. We discuss some of the limitations of the workshop conclusions and suggest a simple analysis of the performance differences that might be expected between short- and long-pulse sources both of which exploit coupled moderators.

1. Results from the Berkeley Workshop[1]

The essential results are contained in Table 1. The rows of the table pertain to various types of instruments while the columns describe factors which affect the relative performance of spectrometers and diffractometers at the LPSS and the ILL, which is the benchmark for this comparison.

Total length, L (m) — except for SANS, the total length of each instrument is chosen to provide a wavelength resolution, $\delta\lambda$, that matches that traditionally used at a reactor. For pinhole SANS, the instrument length is dictated by the need for angular resolution that matches that at the reactor. In the case of NSE, the shortest spectrometer one can imagine building at the LPSS still does not have as poor wavelength resolution as is traditionally used at a reactor.

Chopper pulse length, Δt (msec) — in some cases, the 1 msec LPSS pulse is too long to allow the required wavelength resolution to be achieved with a flight path of reasonable length so a pulse-defining chopper must be used.

Incident wavelength bandwidth, $\Delta\lambda$ (Å) — this is the range of wavelengths that is used simultaneously at the LPSS. The maximum possible value of $\Delta\lambda$ is given approximately by 4.T/L where T is the inter-pulse spacing in milliseconds. For all instruments, the counting frame has to be reduced from its nominal value of 16.7 msec (for a 60 Hz source) to account for penum-

---

Table 1

Spectrometer Type	Equiv ILL Instr.	Total Length (m)	Chopper Δt (msec)	§ Δλ(Å)	§§ δλ(Å)	TOF Gain	¶ Relative Incident Δα	¶¶ Relative Detected Δα	* Relative Flux	** Relative Dyn. Rnge.	1 MW LPSS Performance
Small Angle Scattering											
– 21 m flight path; 10 Å wavelength	D22	21	-	3	1.2	2.5	1	1	0.25		0.6 x ILL
– 21 m flight path; 6 Å wavelength	D22	21	-	3	0.7	4.3	1	1	0.25		1 x ILL
Reflectometer	D17	60	-	1	0.07	15	1	1	0.25		3.5 x ILL
Powder Diffraction											
Low Resolution	D7	40	0.375	1.6	0.04	40	0.2	1	0.075		0.6 x ILL
Medium Resolution	D16	40	0.019	1.6	0.002	800	0.2	10	0.004		6 x ILL
High Resolution	D2B	160	0.02	0.4	0.0005	800	0.2	10	0.003		5 x ILL
Amorphous Material Diffraction	D4	40	0.019	1.6	0.002	800	0.2	1	0.004		0.6 x ILL
Single Crystal Diffraction											
Laue Diffraction		20	-	3.2	0.2	16	1	0.5	0.2		1.5 x ILL
Diffuse Scattering	D7	20	-	3.2	0.2	16	1	1	0.2		3 x ILL
High Resolution Inelastic Scattering											
– multi-chopper spectrometer	IN5						1	1	4	0.5 - 1.0	2 - 4 x ILL
– time focussed TOF spectrometer	IN6						1	1	3.2	0.5	1.6 x ILL
– backscattering (1 µeV resolution)	IN10	92	0.025	0.7	0.001	700	1	1	0.006	0.07 - 1.0	0.25 - 4 x ILL
– backscattering with MUSICAL mono.		92	0.025	0.7	0.001	700	1	1	0.006	1	4 x ILL
Neutron Spin Echo	IN15	16	-	4	1	4	1	1	0.25		1 x ILL
S(Q,E) Spectroscopy (2% resol)	IN4C	15	0.01	4.2	0.003	1400	1	1	0.002	0.2 - 0.8	0.7 - 2.5 x ILL
S(Q,E) Spectroscopy (20% resol)	IN4C	15	0.5	4.2	0.13	32	1	1	0.1	0.25 - 1.0	0.8 - 3.2 x ILL
Conventional Three Axis Machines											
Cold Neutron TAS	IN14		-			1	1	1	0.4		0.4 x ILL
Thermal/Hot Neutron TAS	IN8/IN1		-			1	1	1	0.2		0.2 x ILL
Augmented Three Axis Machines											
Multi-Analyser TAS (RITA)		30	0.2	1.85	0.13	14	0.3 - 1	1	0.25		1 - 3.5 x ILL

§ incident-wavelength bandwidth, including chopper penumbra effects (or usable bandwidth if this is smaller)

§§ incident-wavelength resolution (or required resolution if this is larger)

¶ maximum usable incident angular divergence compared to same quantity for reactor experiment

¶¶ maximum usable detected angular divergence compared to same quantity for reactor experiment

* time-average flux on sample for LPSS divided by same quantity for a 60 MW reactor. Flux is averaged over appropriate part of time pulse and harmonically averaged over wavelength bandwidth. This number also includes monochromator, chopper, guide, and filter transmissions.

** relative dynamic range of LPSS and reactor spectrometers if restricted by repetition frequency

bra effects. In one case (the augmented three-axis spectrometer) the counting frame has been reduced even further to avoid contamination from fast neutrons, although this might not be necessary if this spectrometer were to be located on a curved guide. If the useful wavelength bandwidth does not correspond to the entire measurement frame — as, for example, in the case of three axis spectrometers where only one (Q,E) point is measured — it is the useful bandwidth that appears in this column of the table.

Incident wavelength resolution, $\delta\lambda$ (Å) — whether the pulse width used at the LPSS is set by the neutron source or a chopper, the wavelength resolution is given by $\delta\lambda \approx 4.\Delta T/L$. In two cases — SANS and NSE — the wavelength resolution provided by the untailored pulse from the LPSS is too good. In this case, the resolution that would be used in a corresponding experiment at a reactor is entered in the table.

TOF Gain — this is simply the ratio of wavelength bandwidth, $\Delta\lambda$, to wavelength resolution, $\delta\lambda$, and reflects the number of different wavelengths which are used simultaneous at the LPSS. When a pulse-defining chopper is used at the LPSS, the TOF gain is increased from the inverse of the source duty factor (i.e. $1/0.06 \approx 17$) by a factor of $1/\Delta t$. The average flux on the sample is reduced by the same factor.

Relative incident angular bandwidth — this column contains the ratio of the incident angular bandwidth at LPSS to that at a reactor. With the exception of specular neutron reflection, incident angular bandwidth and incident angular collimation are the same, reflecting the fact that, for conventional neutron instruments, one has no method of coding the angle of incidence of neutrons within a divergent beam. Various focusing techniques are used to increase the incident angular bandwidth. At reactors, vertically (and in rare cases, horizontally) curved monochromators provide divergences of up to $5°$ (FWHM). At pulsed sources, optical elements such as converging guides are used to increase angular bandwidth. Such guides are limited to providing an angular divergence (FWHM) that is about 6 times the nickel critical angle, or $\approx$ $0.6\ \lambda°$. Even for cold neutrons, this divergence is generally less than that which can be obtained with focusing monochromators. However, for some applications — such as specular neutron reflection — increased horizontal and vertical angular bandwidth can be used at a pulsed source, while only increased vertical divergence is available at a reactor without affecting monochromatisation.

Relative detected angular bandwidth — this column contains the ratio of the detected angular bandwidth at the LPSS to that at a reactor. In most cases this ratio is unity, reflecting the fact that the same secondary spectrometer is used at both types of source. However, for wavelength-dispersive powder diffraction at the LPSS, it is sometimes possible to use very high angle detectors which can accept neutrons scattered into a large solid angle without affecting resolution. In the case of Laue diffraction, participants at the Berkeley workshop thought it likely that image plate technology would allow neutrons to be detected within a solid angle that is about twice as large as could be detected with conventional detectors at a pulsed source.

Relative flux on sample — this column contains the ratio of the time-averaged neutron flux incident on a sample at the LPSS to that at the ILL. There are a number of effects that have to be considered to derive this number:
• the time averaged cold flux of a 1 MW LPSS is 25% of that of the ILL and the time-averaged thermal and hot fluxes are both about 12% of the ILL.
• for those instrument — like IN5 or IN6 — that see the peak flux at the LPSS, the relative cold flux is about 4 times higher at the LPSS than at ILL.

- for those instruments which use a pulse-defining chopper at the LPSS but do not use a chopper at the ILL, the flux on the sample is reduced by the ratio of Δt and the natural pulse length of the source (1 msec). If the pulse-defining chopper cuts off the pulse tails there may be an additional reduction in intensity.
- transmission through monochromators and filters at the reactor and through choppers at the LPSS are considered here, as is guide transmission in appropriate cases.
- the intensity of the incident neutron beam is averaged over the incident wavelength band (the harmonic average turns out to be appropriate [2]).

Relative dynamic range — in some cases, notably for chopper spectrometers such as IN5, IN6, IN10, and IN4C, the 60 Hz repetition rate of the LPSS may yield a dynamic range in energy transfer which is larger than that used at the reactor. Depending on the experiment, this may be a disadvantage for the LPSS.

Overall Performance — the overall performance for neutron scattering relative to ILL is obtained by taking the product: (relative dynamical range) x (relative flux) x (relative detected angular bandwidth) x (relative incident angular bandwidth) x (time-of-flight gain). This number is given in the final column of the Table. The values given are in substantial agreement with those derived at the LBNL workshop.

The relative performances contained in the Table are those that apply to LPSS and ILL instruments with similar resolution in the important dimensions of Q and E space. It is worth emphasizing that the comparisons are for unoptimised instruments — we have simply tried to mimic a reactor experiment at an LPSS without trying to make any qualitative changes that would improve performance.

2. Resolution of LPSS and CW Instruments

The results of the Table assume that it is reasonable to compare instruments which have the same FWHM wavelength resolution, $\delta\lambda$, and that one does not need to account for the different shapes of the wavelength-resolution functions at reactors and the LPSS. To address the effects of pulse shape on wavelength resolution we make use of work by Sivia, Silver, and Pynn [3], who postulated that

$$FOM(\Delta t) = \frac{\phi_p \left|\hat{f}(\omega)\right|^2}{\hat{f}(0)[1 + N_B / N_S]}$$

could be used as a figure of merit when a neutron scattering instrument is used to obtain information on scale $\Delta t = 2\pi/\omega$ from a measurement made with a resolution function f(t) whose Fourier transform is $\hat{f}(\omega)$. In this expression, N_B is the background, N_S is the signal, and ϕ_p is the source flux.

In any neutron scattering instrument, the complete resolution function is obtained by convoluting the various contributions that arise from wavelength uncertainties, collimations etc. Since the FOM is proportional to the squared modulus of the Fourier transform of the resolution function, it will involve a product of terms arising from the various sources of resolution. We may thus compare the performance of instruments whose wavelength resolution functions have different shapes by considering the contribution to the FOM from wavelength resolution alone, provided the other sources of resolution are the same for the instruments we are comparing.

Figure 1 shows two resolution functions which have the same integral intensity and the same FWHM — a Gaussian which is supposed to represent wavelength resolution at a reactor instrument and an Ikeda-Carpenter [4] form for a liquid hydrogen moderator with a decay time constant of 700 µsec, folded with a 1 msec proton pulse to represent the LPSS wavelength resolution. We have evaluated the FOM given above with the background term N_B set to zero for both of these resolution functions and display the results in Fig 2. The horizontal axis in Fig. 2, called ω, is the Fourier inverse of λ. The units are chosen so that one wavelength unit in Fig 1 maps to $\omega = 2\pi$ in Fig. 2. Except for the sharp dip in the LPSS FOM, the two curves are fairly similar for values of $\omega < 2\pi$, indicating that it is reasonable to use the FWHM as a measure of resolution when comparing instruments at a reactor and an LPSS. Thus, the performance Table is expected to be reasonably accurate, in spite of the different shape of the wavelength resolution function at the two types of source.
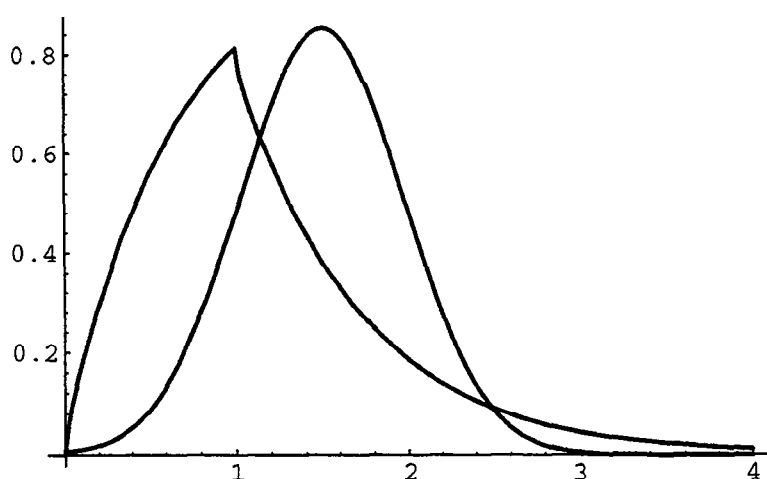

Figure 1. Normalised wavelength resolution functions for a reactor source (Gaussian) and an LPSS.
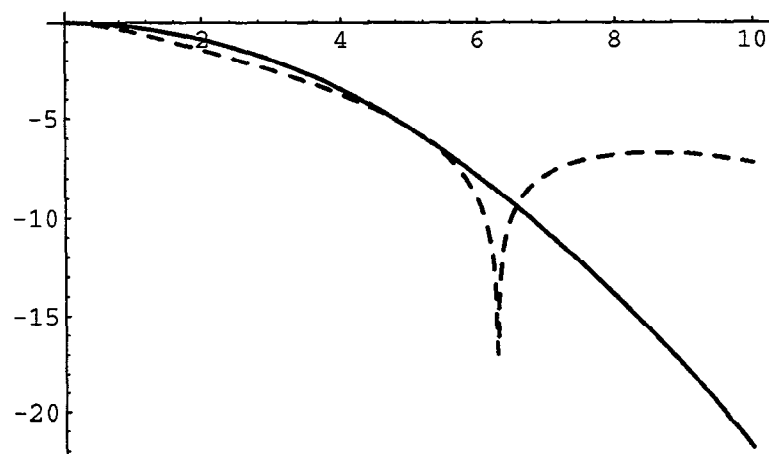

Figure 2. The natural logarithm of the FOM for Gaussian (solid curve) and LPSS (dashed curve) resolution functions is plotted against the Fourier variable ω.

The sharp dip in the FOM for the LPSS deserves comment. It arises from the fact that the proton pulse is assumed to be rectangular in shape. Since this pulse is convolved with the Ikeda-Carpenter form to obtain the overall LPSS pulse shape, the Fourier transform of the LPSS pulse will always have zeroes at multiples of 2π times the width of the proton pulse (taken as unity in plotting Figure 2). This means, of course, that one cannot measure this

Fourier component of a signal. One way to understand this a little better is to imagine a signal composed of equally spaced delta functions — a comb. If the spikes are separated by a distance x and they are measured using a "top hat" resolution function of width x, the measured signal will always be constant, wherever one centers the resolution function.

Before one condemns such a resolution function as useless one should realise that the same effect occurs for a triangular resolution function and that such a shape is highly prized on the spectrometer IN5 at ILL. The point is that although one cannot measure a few localised Fourier components using triangular or rectangular resolution functions, these functions have the advantage of facilitating measurement of high-ω Fourier components. This fact is also clear from Figure 2, where the Gaussian resolution function dies at large values of ω while the envelope of the LPSS resolution function preserves a fairly high value. In a Maximum Entropy type of data analysis [5], one would expect it to be easier to obtain reliable estimates of a few missing Fourier components than to divine the entire high frequency part of the map. In sum, the LPSS resolution function is probably preferable to a standard Gaussian because its leading edge is sharper.

3. Comparing Neutron Scattering Instruments at SPSS and LPSS

It is tempting to ask whether the results shown in the Table can be applied to instruments at an SPSS with coupled moderators. To answer this question, we first examine the pulse shapes that one might expect from SPSS and LPSS. These are shown in Figure 3. The upper part of the Figure shows Ikeda-Carpenter pulses for a liquid hydrogen moderator with a storage time constant of 300 μsec. The lower part displays pulses with a decay constant of 700 μsec. As Russell et al demonstrate elsewhere in these proceedings, the longer time constant is more typical of a coupled, strongly reflected target/moderator system (CSR), while the shorter one might refer to a coupled weakly-reflected system (CWR). Simulations show that the CSR provides about twice the integrated intensity of the CWR and this fact has been accounted for in plotting Figure 3.

The first conclusion one can draw from Figure 3 is that there is little point in strongly coupling the moderators at an SPSS if one is only interested in peak intensity — the peak value changes very little with increasing decay constant. Thus, for an instrument such as IN5, one could equally well use either CSR or CWR target systems at an SPSS. This is not true for the LPSS, which gains with a CSR target system. The reason for this is clear — because the LPSS pulse is derived by convolving a rectangular proton pulse with an SPSS pulse, the long tail of the latter contributes to the peak intensity of the LPSS pulse.

The bottom line from Figure 3 is that an SPSS of a given power and repetition rate is less than a factor of two better than an LPSS of the same power and repetition rate for instruments, like IN5 and IN6, which depend on the peak neutron flux.

Other instruments listed in the Table attain their performance gains over a CW source because they benefit from the full TOF gain given by the inverse duty cycle of the source. While one has to be careful extrapolating this argument to sources with lower and lower duty cycles (cf the article on reflectometry by Fitzsimmons in these proceedings), Figure 3 tells us what happens if the full TOF gain is relevant.

The relative TOF gains for the various pulses are given by the inverse ratios of their FWHMs, at least to the level of approximation in the Table. Measuring the peaks in Figure 3, one finds TOF gains in the ratio SPSS(300):SPSS(700):LPSS(300):LPSS(700) of
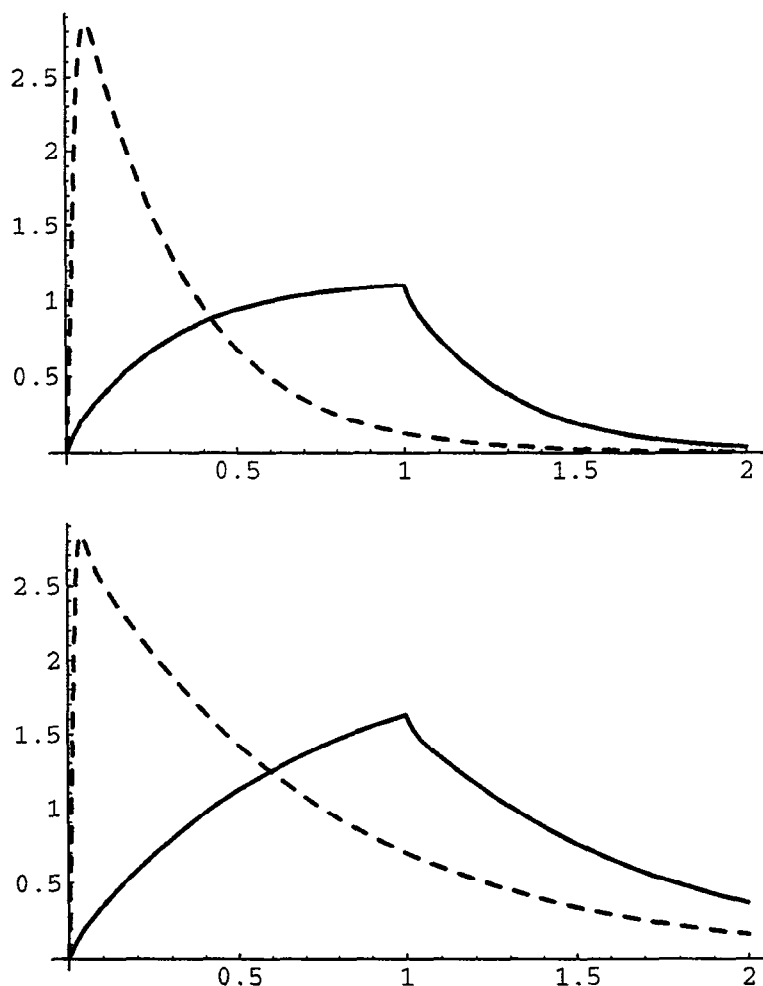
Figure 3. Pulse shapes for SPSS (dotted curve) and LPSS (solid curve) with different time constants. In the upper panel the decay constant is 300 μsec corresponding to a coupled, weakly-reflected target/moderator system (CWR) while in the lower panel the decay constant is 700 μsec, a value more typical of a strongly reflected system (CSR). The integrated intensity of the pulses in the lower panel is twice that of those in the upper panel.

4.2:2.2:1.1:1. The obvious conclusion is that, once more, there is little point in strongly coupling the target/moderator system at an SPSS. By doing so, one loses a factor of almost two in TOF gain and picks up the same factor in integrated intensity. For the LPSS on the other hand, the loss of TOF gain from strong coupling is about 10%, while the gain in overall intensity is a factor of 2.

The bottom line is that for instruments which can benefit from the full TOF gain, the SPSS with either a CWR or CSR target system performs about twice as well as a LPSS of the same power and repetition rate. An important caveat on this statement is that, for equal resolution, the SPSS will have about 4 times the dynamic range per measurement as the LPSS. The whole of this range must contain equally useful information for the performance comparison stated above to be true.

4. Pulse Shapes at SPSS and LPSS

Another instructive exercise is to compare FOM's for SPSS and LPSS pulse shapes. This is done in Figure 4 for a 300 μsec decay constant. Results for a 700 μsec decay constant are very similar. One sees that for measuring structure on a scale of a few times the FWHM of the resolution function (which is what a neutron scattering instrument is generally designed to do), the LPSS pulse shape in to be preferred. This is actually not very surprising when one

336

looks at the relative contributions of the pulse tails to the two peak shapes. Since the integrated intensity produced by both LPSS and SPSS is the same by construction, the FOMs for measuring integrated intensity (i.e. the values of the FOMs at $\omega = 0$) are identical for the two sources. For structure on a scale significantly finer than the FWHM (i.e. for large values of ω), the SPSS line shape is somewhat better because its sharp leading edge preserves high Fourier components of the signal.
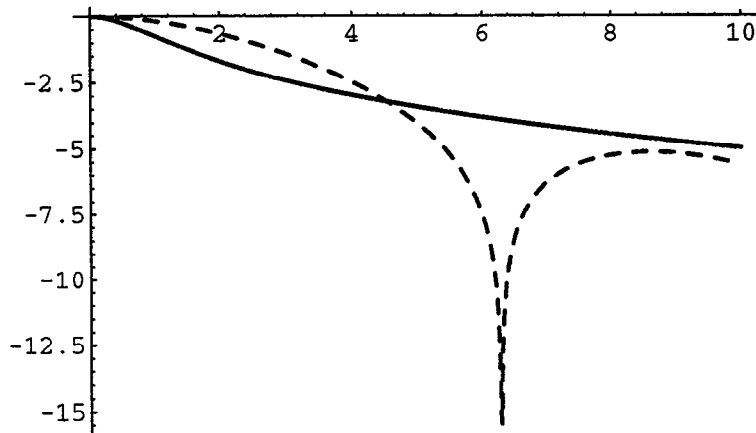

Figure 4. Natural logarithm of the FOM for the SPSS (solid line) and LPSS (dashed line).

Figure 5 shows the FOMs for SPSS and LPSS pulse shapes with 700 μsec decay constant on a linear (as opposed to logarithmic) scale. Recalling that the FOM is inversely proportional to the measurement time required to achieve a given accuracy, one sees that for measuring structure on a scale of two or three times the FWHM of the resolution function (i.e. for values of 2 to 3 on the abscissa of Figure 5), the LPSS out-performs the SPSS by a factor of two or more, effectively canceling the TOF gain noted above for the SPSS.
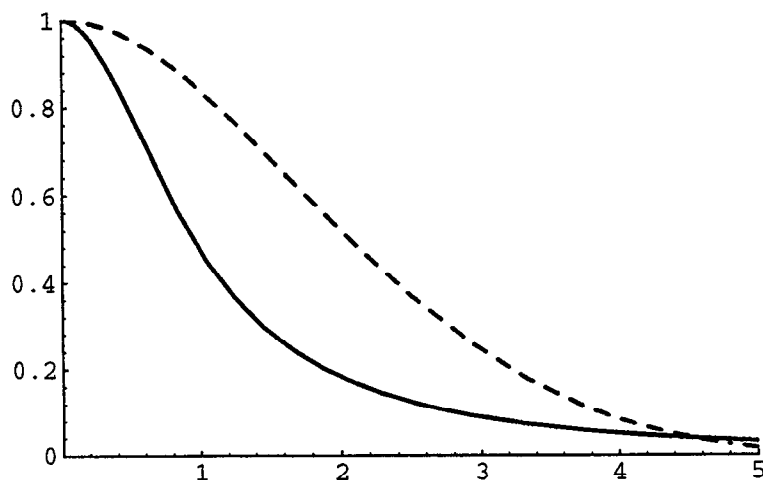

Figure 5. FOMs for SPSS (solid line) and LPSS (dashed line) on a linear scale. A 700 μsec decay constant was used for both pulses.

It is worth noting that the LPSS offers in principle, the possibility of tuning the FOM by tailoring the shape of the proton pulse, a problem we will treat in more detail in a forthcoming paper.

We have chosen to use the Ikeda-Carpenter form for the pulse shape at a spallation source because it provides a simple analytic expression that is easily Fourier transformed and integrated. However, we do not expect our quantitative results to depend very strongly on this

choice because it mimics rather well the exponential tail of the pulse — at least out to a time of order the proton pulse width at an LPSS. A minor change in pulse shape will not affect our qualitative conclusion that the effects of pulse tails on resolution need to be carefully considered in the design of both LPSS and SPSS and that these effect may substantially modify simple minded comparisons based only on peak flux arguments.

5. Conclusion

We have shown that simple scaling arguments involving few variables can be used to provide a first approximation to the comparison of instrument performance at LPSS and CW sources. In addition, we have demonstrated that a comparison of performance at SPSS and LPSS sources is more complex. It appears that the best target/moderator system for an SPSS designed for low-resolution studies will be a coupled, weakly reflected system. At an LPSS, a coupled, strongly reflected system is preferred. For SPSS and LPSS sources of equal power and repetition rate, the calculations presented here do not predict large performance differences for instruments at the two sources. Nevertheless, detailed Monte Carlo simulations will be required to reach firm, quantitative conclusions.

6. Acknowledgments

7. References

[1] Proceedings of a workshop on the performance of research instrumentation at a 1 MW LPSS held at Lawrence Berkeley National Laboratory in April 1995. [Available from Lee Schroeder at LBNL.]
[2] M. R. Fitzsimmons, Nucl. Instrum. Methods. {To be published.]
[3] D. S. Sivia, R. N. Silver, and R. Pynn, Nucl. Instrum. Methods, A287, 538 (1990)
[4] S. Ikeda and J. M. Carpenter, Nucl. Instrum. Methods, A239, 536 (1985)
[5] E. T. Jaynes, in: Maximum Entropy and Bayesian Methods in Applied Statistics, ed. J.H. Justice (CUP, 1986)